Path integral of the Holstein model with a ϕ^4 on-site potential

Marco Zoli*
Dipartimento di Fisica, Istituto Nazionale Fisica della Materia, Università di Camerino, 62032 Italy
(Received 5 August 2005; revised manuscript received 16 September 2005; published 8 December 2005)

We derive the path integral of the semiclassical, one-dimensional anharmonic Holstein model, assuming that the electron motion takes place in a bath of nonlinear oscillators with quartic on-site hard (and soft) potentials. The interplay between the *e-ph* coupling and anharmonic force constant is analyzed both in the adiabatic and antiadiabatic regime. In the latter we find much larger anharmonic features on the thermodynamic properties of low energy oscillators. Soft on-site potentials generate attractive centers at large amplitude oscillator paths and contribute to the anomalous shape of the *heat capacity over temperature* ratio in the intermediate to low T range. This anharmonic lattice effect is superimposed to the purely electronic contribution associated with a temperature-dependent hopping with variable range inducing local disorder in the system.

DOI: 10.1103/PhysRevB.72.214302 PACS number(s): 71.38.−k, 63.20.Ry, 31.15.Kb

I. INTRODUCTION

There is at present a large interest in the effects of a strong electron-phonon coupling in a number of systems ranging from dimer molecular junctions[1] to carbon nanotubes,[2] from organic molecular crystals,[3] to DNA (Ref. 4) and cuprate superconductors.[5,6] Several theoretical studies have focused on the interplay between *e-ph* coupling and nonlinearities in the framework of the Holstein model[7,8] investigating the phase diagram both in the adiabatic[9] and the antiadiabatic regime. Mainly in the latter, anharmonic effects are believed to be large[10] thus offering a picture to explain the high T_c of binary alloys such as superconducting MgB_2 with a small Fermi energy and sizeable *e-ph* coupling.[11]

The path integral formalism provides a powerful method to study quantum systems in which a particle is nonlinearly coupled to the environment.[12–14] A previous path integral analysis[15] has pointed out how the phonon dispersion, which has to be taken into account in the computation of the ground state properties of the Holstein Hamiltonian,[16–18] induces nonlocal *e-ph* correlations that renormalize downwards the effective coupling and ultimately broaden the size of the polaronic quasiparticle. This explains why the polaron mass in a dispersive Holstein model[19] is lighter than in a dispersionless model.[20] Also the thermodynamics of the Holstein Hamiltonian can be computed within a dispersive model that accounts for the lattice structure.[15]

The Holstein diatomic molecular model was originally cast[21] in the form of a discrete nonlinear Schrödinger equation for electrons whose probability amplitude at a molecular site depends on the interatomic vibration coordinates. The nonlinearities are tuned by the *e-ph* coupling,[22] whose strength drives the crossover between a large and a small polaron state according to the degree of adiabaticity and the dimensionality of the system.[23]

In the Holstein model, the phonon thermodynamics is not affected by *e-ph* induced anharmonicities.[24] This follows from the fact that the Holstein perturbing source current is local in time and it does not depend on the electron path coordinate. As a consequence, in the total partition function, electron and lattice degrees of freedom are disentangled and the latter can be integrated out analytically as far as a harmonic lattice model is assumed. However nonlinearities may arise in Holstein-like systems also by virtue of on-site potentials dependent on the lattice structure and, in principle, independent of the *e-ph* coupling. We are thus led to investigate the thermodynamics of the anharmonic Holstein model with a quartic on-site potential, which may be repulsive or partly attractive according to the sign of the force constant and the amplitude of the lattice displacement paths. The path integral approach permits us to monitor the physical properties for any value of the coupling strengths.[25] The presence of a ϕ^4 potential may, in turn, affect also the *e-ph* interactions and sinergically interfere on the equilibrium properties of the system. This is the focus of the present paper. Section II presents the Hamiltonian model, while the path integral method is briefly described in Sec. III. The derivation of the total partition function of the system is presented in Sec. IV, and Sec. V contains the discussion of the physical results. The conclusions are drawn in Sec. VI.

II. THE ANHARMONIC HOLSTEIN MODEL

We consider the one-dimensional anharmonic Holstein Hamiltonian consisting of (i) one electron hopping term; (ii) an interaction which couples the electronic density ($f_l^\dagger f_l$) to the lattice displacement u_l at the l-site, and (iii) a bath of N identical dispersionless anharmonic oscillators with mass M and frequency ω:

$$H = H^e + H^{e\text{-}ph} + H^{ph},$$

$$H^e = -t \sum_{\langle l,m \rangle} f_l^\dagger f_m,$$

$$H^{e\text{-}ph} = \bar{g} \sum_{l=1}^{N} u_l f_l^\dagger f_l,$$

$$H^{ph} = \frac{M}{2} \sum_{l=1}^{N} (\dot{u}_l^2 + \omega^2 u_l^2) + \frac{\delta}{4} \sum_{l=1}^{N} u_l^4,$$

$$\bar{g} = g\sqrt{2M\omega}, \tag{1}$$

the sum $\langle,\rangle$ is over z nearest neighbors and t is the tight binding overlap integral. g is the *e-ph* coupling in units of $\hbar\omega$. Choosing the atomic mass M of order 10^4 times the electron mass, we get $\bar{g} \simeq 1.1456 \times g\sqrt{2\hbar\omega}$ (meV Å^{-1}), where $\hbar\omega$ is given in meV. δ, in units of meV Å^{-4}, controls the strength of the nonlinearities and determines whether the on-site potential $V(u_l) = M\omega^2 u_l^2/2 + \delta u_l^4/4$ is hard ($\delta > 0$) or soft ($\delta < 0$). In the latter case, $V(u_l)$ attains the maximum at $u_l^2 = M\omega^2/|\delta|$ and the inflection point occurs at $u_l^2 = M\omega^2/3|\delta|$. The condition $|\delta| u_l^2 > 2M\omega^2$ yields an attractive on-site potential. Then, the range of the atomic path amplitudes generating attractive scattering centers depends on the value of the anharmonic force constant. For $|\delta| > 2M\omega^2$ the potential becomes attractive for a portion of large amplitude atomic paths while small amplitude paths weigh the repulsive range.

In the following computation of the electron path integral coupled to the anharmonic oscillator, after setting the potential parameters, we select at any temperature the class of atomic paths that mainly contribute to the Euclidean action. As the distribution of the path amplitudes has a cutoff on the scale of the lattice constant, say, i.e., $u_l^2 < 1$ Å^2, the on-site potentials are always bound from below also in the attractive cases.

III. THE PATH INTEGRAL METHOD

The Holstein Hamiltonian in (1) can be mapped onto the time scale according to space-time mapping techniques extensively described in previous works[15,26,27] and hereafter outlined.

Defining $x(\tau)$ and $y(\tau')$ as the electron coordinates at the l and m lattice sites, respectively, H^e in (1) transforms into

$$H^e(\tau,\tau') = -t[f^\dagger(x(\tau))f(y(\tau')) + f^\dagger(y(\tau'))f(x(\tau))], \tag{2}$$

where τ and τ' are continuous variables ($\in[0,\beta]$), with β being the inverse temperature. After setting $\tau' = 0$, $y(0) \equiv 0$ and taking the thermal averages for the electron operators over the ground state of the Hamiltonian, one gets the average electron hopping energy per lattice site:

$$h^e[x(\tau)] \equiv \frac{\langle H^e(\tau)\rangle}{N} = -t\{G[-x(\tau),-\tau] + G[x(\tau),\tau]\}, \tag{3}$$

where $G[x(\tau),\tau]$ is the electron propagator at finite temperature.

By treating the lattice displacements in (1) as $\tau-$ dependent classical variables, $u_l \to u(\tau)$, we obtain from $H^{e\text{-}ph}$ in (1) the averaged *e-ph* energy per lattice site, which is identified as the perturbing source current $j(\tau)$ in the path integral method:

$$j(\tau) \equiv \frac{\langle H^{e\text{-}ph}(\tau)\rangle}{N} = \bar{g}u(\tau). \tag{4}$$

As the Hamiltonian model assumes a set of identical oscillators we study the path integral for the electron coupled to a single anharmonic oscillator of the bath. The path integral reads

$$\langle x(\beta)|x(0)\rangle = \int Dx(\tau)\exp\left[-\int_0^\beta d\tau\, E(x(\tau))\right] \times \int Du(\tau)\exp\left[-\int_0^\beta d\tau\, O(u(\tau))\right],$$

$$E(x(\tau)) = \frac{m_e}{2}\dot{x}^2(\tau) + h^e(x(\tau)),$$

$$O(u(\tau)) = \frac{M}{2}[\dot{u}^2(\tau) + \omega^2 u^2(\tau)] + \frac{\delta}{4}u^4(\tau) + j(\tau), \tag{5}$$

where the kinetic term (m_e is the electron mass) is normalized by the functional measure of integration over the electron paths.

Since the electron hopping does not induce a shift of the oscillator coordinate, the Holstein *e-ph* interactions are local in time and, in the semiclassical treatment, the source current $j(\tau)$ is independent of the electron path. As a consequence, oscillator and electron coordinates appear disentangled in (5) while the coupling occurs through the parameter $\bar{g}$.

IV. THE PARTITION FUNCTION

The quantum statistical partition function Z_T is derived by integrating (5) after imposing periodicity conditions, β is the period, both on the electron and oscillator paths:

$$Z_T = \int dx\langle x(\beta)|x(0)\rangle = Z_{el} \times Z_{osc},$$

$$Z_{el} = \oint Dx(\tau)\exp\left(-\int_0^\beta d\tau\, E(x(\tau))\right),$$

$$Z_{osc} = \oint Du(\tau)\exp\left[-\int_0^\beta d\tau\, O(u(\tau))\right], \tag{6}$$

where $\oint Dx(\tau)$ and $\oint Du(\tau)$ are the functional measures of integration.

The electronic contribution Z_{el} is computed by expanding the paths in Fourier components

$$x(\tau) = x_o + \sum_{m=1}^{M_F}[r_m\cos(\nu_m\tau) + s_m\sin(\nu_m\tau)],$$

$$r_m = 2\,\mathrm{Re}\,x_m,$$

$$s_m = -2\,\mathrm{Im}\,x_m,$$

$$\nu_m = 2m\pi/\beta, \tag{7}$$

and taking the following measure of integration:

$$\oint Dx(\tau) \equiv \frac{\sqrt{2}}{(2\lambda_{m_e})^{(2M_F+1)}} \int_{-\infty}^{\infty} dx_o \times \prod_{m=1}^{M_F} (2\pi m)^2 \int_{-\infty}^{\infty} dr_m \int_{-\infty}^{\infty} ds_m,$$

$$\lambda_{m_e} = \sqrt{\pi\hbar^2\beta/m_e}. \tag{8}$$

The cutoffs over the Fourier coefficient integrations have to ensure proper normalization of the kinetic term in the absence of hopping processes. Thus Z_{el} transforms into

$$Z_{el} \simeq \frac{\sqrt{2}}{(2\lambda_{m_e})^{(2M_F+1)}} \int_{-\Lambda/2}^{\Lambda/2} dx_o \prod_{m=1}^{M_F} \int_{-\Lambda}^{\Lambda} dr_m \int_{-\Lambda}^{\Lambda} ds_m \times \exp\left(-\frac{\pi^3}{\lambda_{m_e}^2} \sum_{m=1}^{M_F} m^2 (r_m^2 + s_m^2) - \int_0^{\beta} d\tau\, h^e(x(\tau)) \right) \tag{9}$$

with $\Lambda \propto \lambda_{m_e}$[27] indicating that large amplitude electron paths have to be selected at low temperatures where the quantum effects are larger. Two Fourier components $M_F=2$ suffice to attain stable results as $h^e(x(\tau))$ depends smoothly on the electron path. The hopping term accounts for the deviation from the Gaussian behavior. Numerical analysis shows that, for any choice of path parameters, $h^e(x(\tau))$ decreases by decreasing the temperature but its overall contribution to the electron action is substantial also at low T.

Let us focus now on the anharmonic oscillator term Z_{osc}. The oscillator path is expanded in N_F Fourier components

$$u(\tau) = u_o + \sum_{n=1}^{N_F} [a_n \cos(\omega_n \tau) + b_n \sin(\omega_n \tau)] \tag{10}$$

with Matsubara frequencies $\omega_n = 2n\pi/\beta$ and coefficients $a_n \equiv \mathrm{Re}\, u_n$, $b_n \equiv -\mathrm{Im}\, u_n$ satisfying the conditions $a_n = a_{-n}$ and $b_n = -b_{-n}$. The latter are consistent with the choice of real paths and simplify the following τ integration of the on-site potential.

Note that the periodicity property $u(\tau) = u(\tau+\beta)$ would be fulfilled also by taking the very a_n coefficients in (10).[28] However, such a choice would not permit fitting, with accuracy, the harmonic oscillator partition function, which is known exactly: $Z_h = [2\sinh(\beta\omega/2)]^{-1}$. In fact, in the path integral method, the harmonic partition function Z_h^{PI} reads

$$Z_h^{PI} = \oint Du(\tau) \exp\left[-\int_0^{\beta} d\tau \left(\frac{M}{2} [\dot{u}^2(\tau) + \omega^2 u^2(\tau)] \right) \right] \tag{11}$$

and taking the functional measure

$$\oint Du(\tau) \equiv \frac{\sqrt{2}}{(2\lambda_M)^{(2N_F+1)}} \int_{-\infty}^{\infty} du_o \times \prod_{n=1}^{N_F} (2\pi n)^2 \int_{-\infty}^{\infty} da_n \int_{-\infty}^{\infty} db_n \tag{12}$$

with $\lambda_M = \sqrt{\pi\hbar^2\beta/M}$, one gets from (10)–(12):

$$Z_h^{PI} = \frac{1}{\beta\omega} \prod_{n=1}^{N_F} \frac{(2n\pi)^2}{(2n\pi)^2 + (\beta\omega)^2}. \tag{13}$$

Instead, by dropping the b_n terms in (10) and (12), one would get the square root of the product series in (13), which does not yield a reliable fit of Z_h even for large N_F. Note that at high T, the condition $2n\pi \gg \beta\omega$ is fulfilled for small integers n, hence the main contribution to Z_h^{PI} is given by the $1/\beta\omega$ factor that stems from the $\int du_o$ in (12). This is consistent with the expectation that high T paths are well approximated by their β-averaged value u_o whereas fluctuation effects become increasingly relevant towards the low-T regime in which N_F rapidly grows. N_F clearly varies also with the oscillator energy while the shape of $N_F(\omega, T)$ may differ according to the harmonic function (Z_h, harmonic free energy or specific heat) one chooses to fit.

The anharmonic partition function Z_{osc} in (6) can be worked out analytically using (10) and (12) and performing the time integration of the oscillator functional $O(u(\tau))$. This permits us to get an insight into the role of the nonlinear terms. The lengthy calculation yields

$$Z_{osc} = \frac{\sqrt{2}}{(2\lambda_M)^{(2N_F+1)}} \int_{-\infty}^{\infty} du_o \exp(-\beta\bar{g}u_o - \kappa u_o^2 - \beta\delta u_o^4/4) \times \prod_{n=1}^{N_F} (2\pi n)^2 \int_{-\infty}^{\infty} da_n \exp\left[-\sum_{n=1}^{N_F} \left((\gamma_n + 3\beta\delta u_o^2/4) a_n^2 + \frac{\beta\delta u_o}{2} \sum_{m=1}^{N_F} c(n,m) + \frac{\beta\delta}{16} \sum_{m,p=1}^{N_F} d(n,m,p) \right) \right] \times \int_{-\infty}^{\infty} db_n \exp\left[-\sum_{n=1}^{N_F} \left((\gamma_n + 3\beta\delta u_o^2/4) b_n^2 + \frac{3\beta\delta u_o}{2} \sum_{m=1}^{N_F} e(n,m) + \frac{\beta\delta}{16} \sum_{m,p=1}^{N_F} [6f(n,m,p) - g(n,m,p)] \right) \right],$$

$$\kappa = \pi(\beta\omega)^2/2\lambda_M^2,$$

$$\gamma_n = \pi[(2\pi n)^2 + (\beta\omega)^2]/4\lambda_M^2,$$

$$c(n,m) = a_n a_m (a_{n+m} + a_{n-m}),$$

$$d(n,m,p) = a_n a_m a_p (a_{n+m+p} + a_{n-m+p} + a_{p-n-m} + a_{p-n+m}),$$

$$e(n,m) = a_n b_m (b_{n+m} - b_{n-m}),$$

$$f(n,m,p) = a_n a_m b_p (b_{n+m+p} + b_{n-m+p} + b_{p-n-m} + b_{p-n+m}),$$

$$g(n,m,p) = b_n b_m b_p (b_{n+m+p} - b_{n-m+p} + b_{p-n-m} - b_{p-n+m}). \quad (14)$$

In $c(n,m)$ the coefficients a_j $(j=n+m,n-m)$ vanish if $j \leq 0$ or $j > N_F$. In $d(n,m,p)$, $a_k \neq 0$ $(k=n+m+p,\ n-m+p,\ p-n-m,\ p-n+m) \Leftrightarrow 1 \leq k \leq N_F$. Analogous conditions hold for the coefficients $b_{j(k)}$ in the $e(n,m)$, $f(n,m,p)$, and $g(n,m,p)$ functions.

Note that the effective *e-ph* coupling $\bar{g}$ is associated only to the τ-independent component u_o, that is to the β-averaged displacement path.[15] This follows from the fact that the perturbing source current is nonretarded in the Holstein model as a consequence of the local nature of the *e-ph* interaction.

The quartic potential induces a strong mixing of the Fourier components of the path that highly complicates the numerical problem. Thus the value of N_F appears to be crucial in the computation. We determine $N_F(\omega,T)$ by fitting (with an accuracy of 2×10^{-2}) the exact harmonic free energy $[F_h=-\ln(Z_h)/\beta]$, through the path integral harmonic free energy F_h^{PI} obtained from (13). As an example, for the oscillator with $\omega=20$ meV, $N_F(T=10\ \mathrm{K})=59$ and $N_F(T=200\ \mathrm{K})=8$.

Inspection of (14) offers the key to performing reliable path integrations according to the sign of the ϕ^4 potential. At high temperature, a large contribution to Z_{osc} is expected to come from the paths having u_o which maximizes $\exp(\kappa f(u_o))$ with $f(u_o)=-(au_o+u_o^2+bu_o^4)$, $a \equiv \beta\bar{g}/\kappa$; $b \equiv \beta\delta/4\kappa$. In general, we find that for a hard (soft) potential, the du_o integration has to be carried out along the $u_o<0(u_o>0)$ axis, with cutoff $|u_o|_{max} \sim 0.6/\sqrt{\kappa}$. This permits us to include the set of paths that mainly contribute to the Euclidean oscillator action. On the Fourier coefficients integrals $\int da_n$, $\int db_n$, we set the cutoffs $|a_n|_{max}$, $|b_n|_{max} \sim 0.6/\sqrt{\gamma_n}$ both for hard and soft potentials, thus achieving numerical convergence and correct computation of the Gaussian integrals once the nonlinearities are switched off. It turns out [see the definitions in (14)] that the cutoffs on the oscillator path integration are increasing functions of temperature ($\propto\sqrt{T}$) consistently with the physical expectations of large amplitude displacements at high T. As the path displacements encounter an upper limit due to the cutoffs, $u(\tau) \leq |u_o|_{max} + 2\Sigma_{n=1}^{N_F} |a_n|_{max}$, the distribution of on-site potentials has a lower limit also in the case of soft and attractive nonlinearities. This avoids numerical divergences and makes the problem physically meaningful.

V. RESULTS

We test the relevance of the nonlinearities on the equilibrium thermodynamics of the system and present the calculation for the heat capacity in the intermediate to low temperature range.

Figures 1 show the behavior of a low energy ($\omega=20$ meV) oscillator without ($g=0$) and with ($g=2,4$) coupling to the electronic subsystem in the adiabatic regime: $t/\omega=5$. Figures 1(a) and 1(b) assume an anharmonic potential with positive quartic force constant $\delta=10^3$, 10^4 meV Å^{-4}, respectively. Also the harmonic heat capacity is reported on for comparison. The hard potential lifts the free energy over the harmonic values with a more pronounced enhancement at increasing T and for larger δ. The effect on the free energy second derivative is however scarce and essentially consists in a slight increase (decrease) of the heat capacity at low (high) temperatures [see Fig. 1(a)]. The reduction of the heat capacity (with respect to the harmonic plot) at intermediate and high T is more evident in Fig. 1(b) where the quartic force constant is larger. This result is in accordance with diagrammatic perturbative treatments of the anharmonic crystals which predict negative contributions to the constant volume specific heat arising from positive force constants in the quartic potential.[29,30] The *e-ph* coupling strength also tends to decrease the oscillator heat capacity but the overall effect is small as the insets in the figures show: in fact, the electronic term dominates the total heat capacity C and the oscillator contribution is not distinguishable in the plots of the C over temperature ratios versus T. The low temperature upturn is due to the large electron energy term in (9) and precisely ascribable to the feature of the variable range (on the τ scale) of the electron hopping, captured by the path integral formalism.[27]

The cases of a soft on-site potential are reported on in Fig. 1(c) with $\delta=-10^3$ meV Å^{-4} and Fig. 1(d) with $\delta=-10^4$ meV Å^{-4}. The characteristic potential parameter is $M\omega^2/|\delta| \simeq 0.5$ and 0.05 Å^2, respectively. The potential $V(u(\tau))=M\omega^2 u(\tau)^2/2+\delta u(\tau)^4/4$ is attractive for those paths such that $u(\tau)^2 > 2M\omega^2/|\delta|$.

At any T, we integrate over a distribution of time-dependent potentials. Thus, at a given lattice site, the electron may experience an attractive or repulsive scattering center according to the size of the atomic path. As an example, at $T=200$ K, we get a maximum path u_{max} such that $u_{max}^2 \sim 0.15$ Å^2. This guarantees that $V(u(\tau))$ is generally repulsive in Fig. 1(c) and attractive for a broad class of paths in Fig. 1(d).

The effects on the oscillator heat capacity are twofold: (i) the soft potential enhances the heat capacity mainly in the low T range with respect to the hard potential and this feature is much more pronounced in Fig. 1(d); (ii) the trend of the *e-ph* coupling is opposite to that observed in Figs. 1(a) and 1(b): now by increasing the g values one gets higher heat capacities although the size of this effect is small on the scale of the electronic terms in the adiabatic regime as revealed by the C/T plots in the insets.

Let us come to the antiadiabatic regime ($t/\omega=0.5$) discussed in Figs. 2, where a low harmonic energy ($\omega=10$ meV) is assumed to emphasize the size of the anharmonicity together with a very narrow electron band. A hard on-site potential with $\delta=10^3$ meV Å^{-4} is taken in Fig. 2(a): the shape of the oscillator heat capacity signals the effects of the nonlinearities, which flatten the curve at intermediate T and enhance the heat capacity also at low T with respect to the corresponding case of Fig. 1(a). As the Debye temperature is now smaller [than in Fig. 1(a)], the hard anharmonicity decreases the constant volume heat capacity with respect to the harmonic plot over a broader temperature range.

The *e-ph* coupling also plays a minor role in antiadiabatic

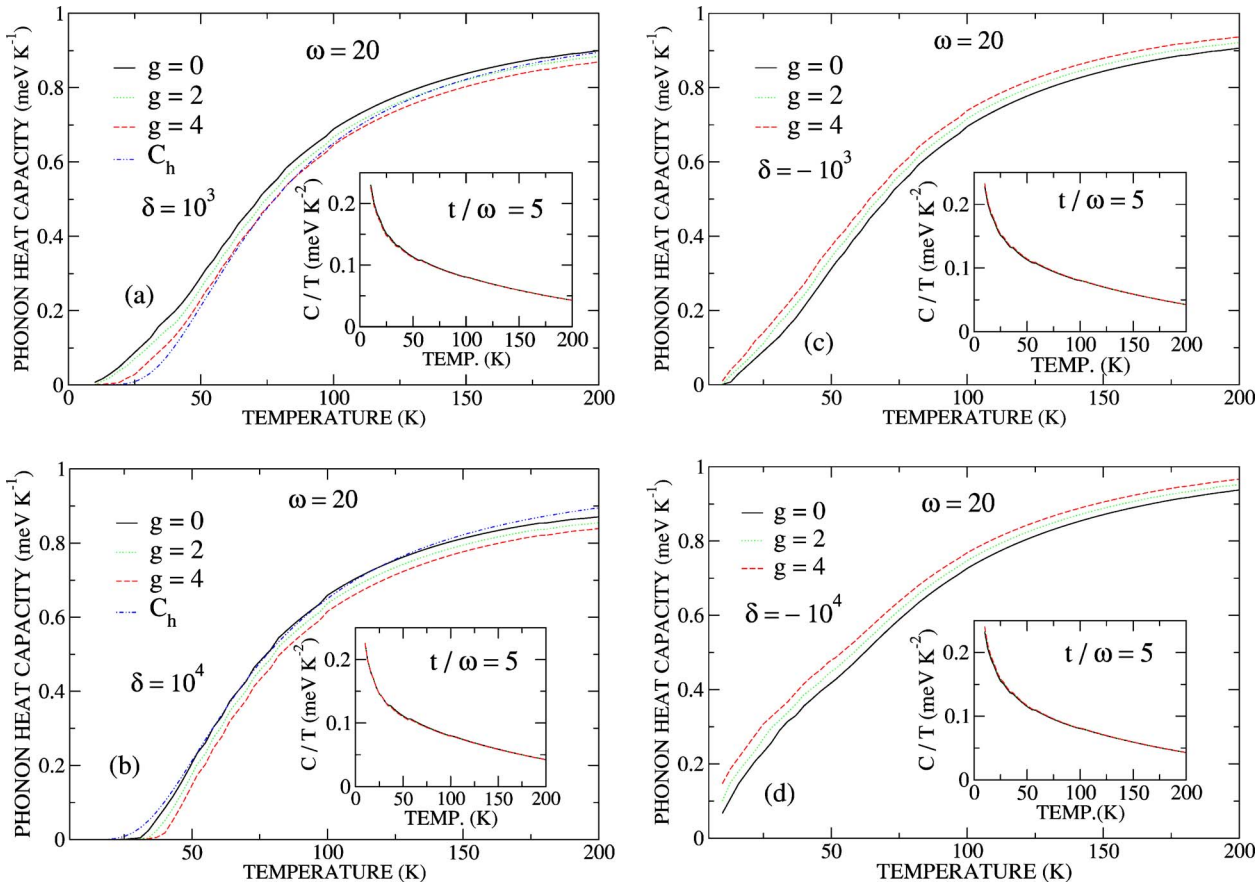

FIG. 1. (Color online) Anharmonic oscillator heat capacities versus temperature for three values of *e-ph* coupling g and oscillator energy ω=20 meV. (a) Hard potential with force constant δ=10^3 meV Å^{-4}; (b) δ=10^4 meV Å^{-4}; (c) soft potential with δ=-10^3 meV Å^{-4}; (d) δ =-10^4 meV Å^{-4}. The harmonic heat capacity is plotted in (a) and (b) for comparison. The insets show the total (electronic plus anharmonic oscillator) heat capacity over temperature ratios in the adiabatic regime t/ω=5.

conditions. The anharmonic contribution is visible in the total heat capacity as the inset makes evident although the dominant electronic feature persists in the low T upturn of C/T. In Fig. 2(b), we assume g=2 and consider two cases of soft potential: the oscillator anharmonicity becomes relevant and such to modify the shape of the anomalous upturn in the total heat capacity. An enhancement of the C/T values is observed at intermediate and low T and, in the case of the largest $|\delta|$ generating a soft attractive potential, the oscillator heat capacity C_{osc} yields an upturn in C_{osc}/T independently of the electronic term.

VI. CONCLUSIONS

We have studied the path integral of the one-dimensional nonlinear Holstein model in which a set of dispersionless oscillators provides the environment for the electron. The model is semiclassical as the lattice displacements are treated classically while the electron operators are thermally averaged over the ground state Hamiltonian. The *e-ph* coupling of the model is local and generates a perturbing current which linearly depends on the oscillator path amplitude $u(\tau)$ where τ is the time (or inverse temperature) of the Matsubara Green functions formalism. The anharmonicity on the lattice site is modeled through a ϕ^4 potential that may result attractive for a set of displacement paths in the case of a negative quartic force constant (soft potential). We have derived the path integral of the interacting system and computed the total partition function selecting, as a function of the temperature ($T \leqslant 200$ K), both the electron and oscillator paths that yield the largest contribution to the action. While quantum electron paths have increasing amplitudes at decreasing temperatures, the atomic displacements are growing functions of T. This relevant physical feature is accounted for in our model as the cutoffs on the electron path integration are proportional to the electron thermal wavelength whereas, on the atomic path integration, we find cutoffs proportional to $\sqrt{T}$.

The oscillator partition function includes the effect of the coupling to the electron subsystem but the on-site anharmonicities play a major role mainly when the potential is soft and the harmonic energy is low. Among the thermodynamic properties we have chosen to present the heat capacity C in view of the upturn in the C/T behavior due to the low T electron hopping tuned by the value of the overlap integral in the Hamiltonian model. The computation is highly time consuming, especially because of the strong mixing of the path Fourier components generated by the nonlinear potential.

In general we find that (i) in the case of a hard quartic potential, switching on the *e-ph* coupling leads to lower free

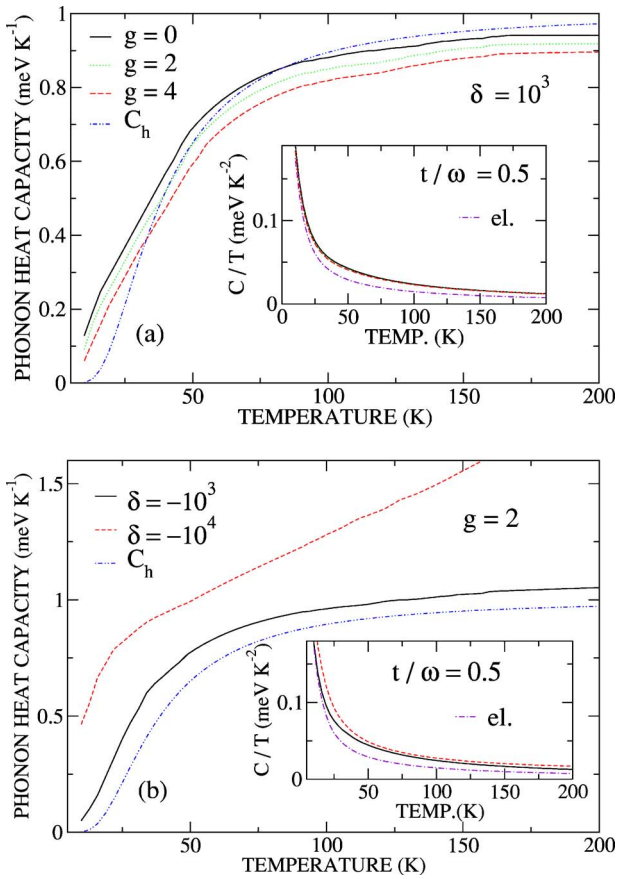

FIG. 2. (Color online) Anharmonic oscillator heat capacities versus temperature in the antiadiabatic regime $t/\omega=0.5$ and oscillator energy $\omega=10$ meV. The harmonic heat capacity is also plotted. (a) Hard potential force constant $\delta=10^3$ meV Å^{-4} with three values of *e-ph* coupling g. (b) Two soft potential force constants at fixed *e-ph* coupling. The insets show the total (electronic plus anharmonic oscillator) heat capacity over temperature ratios. The electronic contribution is plotted separately for comparison.

energy and its second derivative, (ii) when the quartic potential is soft, *e-ph* coupling and anharmonicity act sinergically enhancing the thermodynamic functions.

These results can be understood on general physical grounds. In fact, a hard quartic potential shifts the characteristic phonon frequency upwards, thus hardening the spectrum and broadening the size of the quasiparticle. If the *e-ph* coupling is enhanced (independently of the on-site anharmonicity) the magnitude of the source that causes the lattice distortion becomes larger. This further hardens the vibrations and leads to decrease the anharmonic heat capacity over the whole temperature range. Instead, when the quartic potential is soft the phonon frequency is lowered and the oscillator potential well is more flexible. In this case, larger *e-ph* coupling strengths favor the self-trapping of quasiparticles with heavier effective masses. This is physically equivalent to softening the phonon spectrum and enhancing the heat capacity.

The electron contribution to the heat capacity is dominant in the adiabatic regime whereas antiadiabatic systems are expected to present significant anharmonic corrections. In fact, in the antiadiabatic regime the quasiparticle is a small size object on the lattice scale and the electron energy associated with the overlap integral is small. Thus, this regime proposes a physical picture in which the electron hardly hops from site to site and its effective mass becomes heavier on the scale of the atomic mass. But a potential well generated by "lighter oscillators" is more sensitive to on-site anharmonic effects.

In particular, soft potentials increase the heat capacities over the harmonic values and reinforce the upturn in the C/T versus T plots when the on-site anharmonicity is such as to produce attractive potentials for a set of lattice displacement paths. Since the path amplitudes are larger at high T, soft attractive potentials induce rapidly increasing phonon heat capacities at growing T as shown in Fig. 2(b).

Thus our path integral investigation and the thermodynamical results point to a complex role of the lattice anharmonicities in the one-dimensional Holstein model and suggest that on-site potentials may be experienced as attractive or repulsive according to the temperature and the amplitude of the atomic path. Such potentials may provide scattering centers generating a local disorder whose effect on the system thermodynamics is superimposed on the disorder induced by the hopping of electrons with variable range.

*E-mail address: marco.zoli@unicam.it

[1] G. A. Kaat and K. Flensberg, Phys. Rev. B **71**, 155408 (2005).
[2] L. M. Woods and G. D. Mahan, Phys. Rev. B **61**, 10651 (2000).
[3] K. Hannewald, V. M. Stojanović, J. M. T. Schellekens, P. A. Bobbert, G. Kresse, and J. Hafner, Phys. Rev. B **69**, 075211 (2004).
[4] S. S. Alexandre, E. Artacho, J. M. Soler, and H. Chacham, Phys. Rev. Lett. **91**, 108105 (2003).
[5] T. Schneider, R. Khasanov, K. Conder, and H. Keller, J. Phys.: Condens. Matter **15**, L763 (2003).
[6] A. Lanzara, P. V. Bogdanov, X. J. Zhou, S. A. Kellar, D. L. Feng, E. D. Lu, T. Yoshida, H. Eisaki, A. Fujimori, K. Kishio, J. -I. Shimoyama, T. Noda, S. Uchida, Z. Hussain, and Z. -X. Shen, Nature (London) **412**, 510 (2001).
[7] Y. Zolotaryuk, P. L. Christiansen, and J. J. Rasmussen, Phys. Rev. B **58**, 14305 (1998).
[8] N. K. Voulgarakis and G. P. Tsironis, Phys. Rev. B **63**, 014302 (2001).
[9] K. Ziegler and D. Schneider, J. Phys.: Condens. Matter **17**, 5489 (2005).
[10] L. Boeri, G. B. Bachelet, E. Cappelluti, and L. Pietronero, Phys. Rev. B **65**, 214501 (2002).
[11] T. Yildirim, O. Gülseren, J. W. Lynn, C. M. Brown, T. J. Udovic, Q. Huang, N. Rogado, K. A. Regan, M. A. Hayward, J. S. Slusky, T. He, M. K. Haas, P. Khalifah, K. Inumaru, and R. J. Cava, Phys. Rev. Lett. **87**, 037001 (2001).

[12] R. P. Feynman and A. R. Hibbs, *Quantum Mechanics and Path Integrals* (McGraw-Hill, New York, 1965).
[13] H. Kleinert, *Path Integrals in Quantum Mechanics, Statistics and Polymer Physics* (World Scientific Publishing, Singapore, 1995).
[14] U. Eckern, M. J. Gruber, and P. Schwab, Ann. Phys. **14**, 578 (2005).
[15] M. Zoli, Phys. Rev. B **71**, 184308 (2005).
[16] T. Holstein, Ann. Phys. (N.Y.) **8**, 343 (1959).
[17] H. De Raedt and A. Lagendijk, Phys. Rev. B **30**, 1671 (1984).
[18] M. Zoli, Phys. Rev. B **57**, 10555 (1998).
[19] M. Zoli and A. N. Das, J. Phys.: Condens. Matter **16**, 3597 (2004).
[20] A. S. Alexandrov and P. E. Kornilovitch, Phys. Rev. Lett. **82**, 807 (1999).
[21] T. Holstein, Ann. Phys. (N.Y.) **8**, 325 (1959).
[22] V. M. Kenkre, H.-L. Wu, and I. Howard, Phys. Rev. B **51**, 15841 (1995).
[23] L. C. Ku, S. A. Trugman, and J. Bonča, Phys. Rev. B **65**, 174306 (2002).
[24] M. Zoli, Phys. Rev. B **70**, 184301 (2004).
[25] R. P. Feynman, Phys. Rev. **97**, 660 (1955).
[26] D. R. Hamann, Phys. Rev. B **2**, 1373 (1970).
[27] M. Zoli, Phys. Rev. B **67**, 195102 (2003).
[28] R. P. Feynman, *Statistical Mechanics: A Set of Lectures* (Benjamin, New York, 1972).
[29] D. L. Martin, Can. J. Phys. **65**, 1104 (1987).
[30] M. Zoli, Phys. Rev. B **41**, 7497 (1990).